Cellular and Molecular Life Sciences (2022) 79:452
https://doi.org/10.1007/s00018-022-04480-2

ORIGINAL ARTICLE

Endoplasmic reticulum stress contributes to cisplatin-induced chronic kidney disease via the PERK–PKCδ pathway

Shaoqun Shu[1] · Hui Wang[1] · Jiefu Zhu[2] · Ying Fu[1] · Juan Cai[1] · Anqun Chen[1] · Chengyuan Tang[1] · Zheng Dong[1,3]

Received: 2 April 2022 / Revised: 22 June 2022 / Accepted: 6 July 2022 / Published online: 27 July 2022

Abstract

Background Cisplatin is an effective chemotherapeutic drug, but it may induce both acute and chronic kidney problems. The pathogenesis of chronic kidney disease (CKD) associated with cisplatin chemotherapy remains largely unclear.

Methods Mice and renal tubular cells were subjected to repeated low-dose cisplatin (RLDC) treatment to induce CKD and related pathological changes. The roles of endoplasmic reticulum (ER) stress, PERK, and protein kinase C-δ (PKCδ) were determined using pharmacological inhibitors and genetic manipulation.

Results ER stress was induced by RLDC in kidney tubular cells in both in vivo and in vitro models. ER stress inhibitors given immediately after RLDC attenuated kidney dysfunction, tubular atrophy, kidney fibrosis, and inflammation in mice. In cultured renal proximal tubular cells, inhibitors of ER stress or its signaling kinase PERK also suppressed RLDC-induced fibrotic changes and the expression of inflammatory cytokines. Interestingly, RLDC-induced PKCδ activation, which was blocked by ER stress or PERK inhibitors, suggesting PKCδ may act downstream of PERK. Indeed, suppression of PKCδ with a kinase-dead PKCδ (PKCδ-KD) or *Pkcδ*-shRNA attenuated RLDC-induced fibrotic and inflammatory changes. Moreover, the expression of active PKCδ-catalytic fragment (PKCδ-CF) diminished the beneficial effects of PERK inhibitor in RLDC-treated cells. Co-immunoprecipitation assay further suggested PERK binding to PKCδ.

Conclusion These results indicate that ER stress contributes to chronic kidney pathologies following cisplatin chemotherapy via the PERK–PKCδ pathway.

Keywords Unfolded protein response · Chronic nephrotoxicity · Protein kinase C-δ · Kidney repair

Abbreviations

CKD	Chronic kidney disease
RLDC	Repeated low-dose cisplatin
ER	Endoplasmic reticulum
PKCδ	Protein kinase C-δ
PKCδ-KD	Kinase-dead PKCδ
PKCδ-CF	Active PKCδ-catalytic fragment
AKI	Acute kidney injury
UPR	Unfolded protein response
NF-κB	Nuclear factor-kappa B
FN	Fibronectin
TUDCA	Tauroursodeoxycholic acid
4-PBA	4-Phenylbutyric acid
HE	Hematoxylin–eosin
BUN	Blood urea nitrogen
GFR	Glomerular filtration rate
Mcp-1	Monocyte chemoattractant protein-1
Cxcl1	C–X–C motif chemokine ligand 1
W	Week
M	Month

✉ Chengyuan Tang
tangchengyuan@csu.edu.cn

✉ Zheng Dong
zdong@augusta.edu

[1] Hunan Key Laboratory of Kidney Disease and Blood Purification, Department of Nephrology, The Second Xiangya Hospital of Central South University, Changsha 410011, Hunan, China

[2] Department of Nephrology, Renmin Hospital of Wuhan University, Wuhan, China

[3] Department of Cellular Biology and Anatomy, Medical College of Georgia at Augusta University and Charlie Norwood VA Medical Center, Augusta, GA, USA

Introduction

Cisplatin is widely used as a chemotherapeutic drug to treat various tumors. However, its side effects in normal tissues, particularly nephrotoxicity, limited its clinical use and efficacy [1–14]. Clinically, cancer patients usually receive low, repeated doses of cisplatin to keep chemotherapeutic efficacy and reduce its side effects. Yet, even under this dosing regimen, around 30% of these patients still suffer from acute kidney injury (AKI) [15, 16]. Cisplatin-induced chronic kidney disease (CKD) has also been reported in humans [17]. Experimentally, recent studies have demonstrated that repeated low-dose cisplatin (RLDC) treatment that recapitulates the clinical settings induces renal fibrosis, renal tubular atrophy, and/or atubular glomerulus in mice, suggesting that RLDC treatment induces CKD [18–21]. As cancer survival rates improve, cisplatin-induced CKD will also increase and become a concern for both patients and physicians [17, 22, 23]. However, despite the recognition of cisplatin-related CKD, the mechanisms underlying its pathogenesis remain largely unclear.

Endoplasmic reticulum (ER) stress is a cellular stress state caused by excessive accumulation of misfolded and/or unfolded proteins in the ER lumen. In response to ER stress, mammalian cells mount the unfolded protein response (UPR) involving three sensor proteins, ie. PERK, IRE1, and ATF6-mediated signaling pathways, to restore ER homeostasis [24, 25]. In this regard, upon activation, PERK phosphorylates eIF2α to prevent further unfolded protein accumulation [26]. Activated PERK has also been implicated in regulating nuclear factor erythroid 2-related factor 2 and nuclear factor-kappa B (NF-κB) which play essential roles in regulating redox metabolism, inflammatory processes, and other functions [27–31]. ER stress contributes to the progression of kidney diseases [32–36]. For instance, we recently showed that the persistence of ER stress in renal tubules after renal ischemic injury contributed critically to the development of CKD [35]. However, the function of ER stress in RLDC-related CKD is currently unknown.

Protein kinase C-δ (PKCδ) is widely expressed in many kinds of tissues and cells [37]. Upon intracellular stress, such as DNA damage, ER stress, and /or oxidative stress, PKCδ is activated by phosphorylation on various serine/threonine and tyrosine residues, including Y311 by upstream protein kinases [38, 39]. PKCδ has been reported to have a function in cisplatin-induced AKI [40, 41]. It remains unclear whether PKCδ also contributes to the development of CKD following cisplatin treatment.

In this research, we determined the role and underlying mechanism of ER stress in RLDC-induced CKD. We demonstrated that ER stress was induced by RLDC in kidney tubular cells in vivo in mice and in vitro in renal proximal tubular cells. Inhibitors of ER stress or PERK given after RLDC treatment attenuated RLDC-induced CKD. Mechanistically, PERK was shown to interact and activate PKCδ to induce a pro-fibrotic and pro-inflammatory phenotype in renal proximal tubular cells. Thus, ER stress, especially PERK, may contribute critically to cisplatin-induced CKD via PKCδ, suggesting a potential kidney protective strategy for cancer patients by targeting this pathway.

Materials and methods

Antibodies and reagents

Primary antibodies including anti-PERK (3192), anti-vimentin (5741), anti-p-PERK (3179S), anti-eIF2α (5324S), and anti-p-eIF2α (3597S) were from Cell Signaling Technology in Boston, USA; anti-Fibronectin (FN) (ab2413), anti-collagen IV (ab6586), anti-alpha smooth muscle Actin (α-SMA) (ab5694), anti-p-PKCδ (ab76181) and anti-PKCδ (ab182126) were from Abcam in Cambridge, UK; anti-F4/80 (GB11027) was from Servicebio in Wuhan, China; anti-GAPDH (10494-1-AP) was from Proteintech in Chicago, USA; anti-collagen I (AF7001) was from Affinity in Jiangsu, China. Cisplatin (H20040813) was from Hansoh Pharma in Jiangsu, China. Tauroursodeoxycholic acid (TUDCA) (S3654) and 4-phenylbutyric acid (4-PBA) (S4125) were from Selleck in Houston, USA. GSK2656157 (5.04651) was from EMD Millipore in Massachusetts, USA. Lipofectamine 3000 (2343152) was from Invitrogen in California, USA.

Animal models

C57BL/6 male mice (8 weeks old) came from SJA Laboratory Animal Corporation in Changsha, China. The mice were housed at the Second Xiangya Hospital of Central South University for 1 week to adapt to the environment with free access to food and water and a 12-h light–dark cycle. The mice were grouped and treated as follows. There were no additional criteria used for including and excluding animals during the experiment.

1. To determine the activation of ER stress during RLDC treatment, mice were subjected to four weekly injections of cisplatin (8 mg/kg) or saline (as the control group) intraperitoneally. The mice injected with saline were killed 1 month after the last saline injection (Ctrl group), and the mice subjected to RLDC treatment were killed 1 week (RLDC − 1 W) or 1 month (RLDC − 1 M) after the last cisplatin injection.

2. To determine the effect of pharmacological inhibition of ER stress with TUDCA or 4-PBA, mice were subjected to four weekly injections of cisplatin (8 mg/kg) (RLDC group) or saline (Ctrl group) intraperitoneally. After the last cisplatin injection, the RLDC mice were randomly divided into 3 groups, which respectively received intraperitoneal injection of 250 mg/kg of TUDCA (RLDC + TUDCA), 20 mg/kg of 4-PBA (RLDC + 4-PBA), or saline (RLDC + saline) daily for 1 week, and each group contained six mice. Similarly, after the last saline injection, the saline-injected control (Ctrl) mice were randomly divided into Ctrl + TUDCA group, Ctrl + 4-PBA group, and Ctrl + saline group, and each group contained 6 mice. The mice were killed 1 month after the last injection of cisplatin or saline.

Immunoblot analysis

Kidney tissues or cells were lysed by 2% sodium dodecyl sulfate buffer with 1% protease inhibitor cocktail from Sigma-Aldrich in Missouri, USA. Proteins from different groups were separated via 8% or 10% sodium dodecyl sulfate–polyacrylamide gels and then transferred to polyvinylidene difluoride membranes. The membranes were incubated sequentially with blocking buffer (5% fat-free milk or bovine serum albumin) at room temperature for 1 h, a primary antibody (1:5000 dilution for anti-GAPDH, 1:3000 dilution for anti-PKCδ and anti-p-PKCδ, and 1:1000 dilution for other primary antibodies) at 4 ℃ overnight and a corresponding secondary antibody (1:5000 dilution) at room temperature for 1 h. In some conditions, the blots were stripped and reprobed for other proteins. The blots were visualized by chemiluminescent substrate from Thermo Fisher Scientific in Massachusetts, USA. Protein band intensity was quantified using ImageJ software (NIH). For densitometry, the signal of the target protein was normalized to the reference protein's signal to determine the ratio.

Hematoxylin–eosin (HE) and Masson trichrome staining

4 μm paraffin-embedded kidney tissue sections underwent deparaffinization and rehydration. HE staining was performed to assess kidney injury and tubular atrophy as previously described [42]. Kidney tubular atrophy was characterized by apparent expansion of the interstitial space, tubule dilation, and necrotic debris in the tubule lumen. Renal tubular atrophy was quantitated by evaluating the percentage of the atrophic tubules in a blinded manner (the person analyzing the staining was blinded to the experimental groups) as follows: 0, no damage; 1, < 25%; 2, 25–50%; 3, 50–75%; 4, > 75%. Masson trichrome staining was performed to assess collagen deposition following standard procedure, and the staining results were quantified by evaluating the percentage of collagen staining positive area in a blinded manner (the person analyzing the staining was blinded to the experimental groups) [42]. For quantification, 10–20 fields were randomly selected from the kidney tissue sections of each mouse to assess the mean value of tubular atrophy and collagen staining positive area. Kidney tissue sections from 6 mice were analyzed in each group.

Blood urea nitrogen (BUN) and serum creatinine

BUN and serum creatinine were analyzed with standard automated enzymatic methods with HITACHI automatic analyzer at the Second Xiangya Hospital.

Glomerular filtration rate (GFR)

GFR was assessed through monitoring FITC-Sinistrin clearance transdermally [43]. Mice were shaved 1 day before monitoring GFR. The GFR monitor (MediBeacon, Germany) was kept on the skin with bilateral adhesive patch and medical tape. Two minutes later, FITC-Sinistrin (70 mg/kg) was injected via tail vein, and the mouse with GFR monitor was placed back in the cage for 1–2 h for measurement. Data were analyzed by Studio software.

Immunohistochemical staining

4 μm paraffin-embedded kidney tissues were deparaffinized and rehydrated. The tissues were then subjected to antigen retrieval by microwave heating in 10 mM sodium citrate buffer (pH 6.0), followed by cooling for at least 1 h. After washing with phosphate buffered saline (pH 7.4), the tissue sections were incubated sequentially with 3% H_2O_2 (10 min at room temperature) and goat serum (1 h at room temperature) for endogenous peroxidase inactivation and blocking. Then, the sections were incubated sequentially with a primary antibody (1:1000 anti-p-PERK and 1:400 anti-F4/80) at 4 °C overnight, and a horseradish peroxidase-conjugated secondary antibody at room temperature for 1 h. The antigen–antibody complex was detected with DAB Kits (Vector Laboratories, California, USA) following the manufacturer's instruction. For quantification, 10–20 fields were randomly selected from the kidney tissue sections of each mouse to assess the mean value of the percentage of positive tubules and the number of positive cells per mm^2 in a blinded manner (the person analyzing the staining was blinded to the experimental groups). Kidney tissue sections from 6 mice were analyzed for each group.

Quantitative real-time PCR

Trizol (CWBIO, Beijing, China) was used to extract RNA from kidney tissues or cells according to the manufacturer's instructions. Taqman RT reagent (TaKaRa, Japan) was used to synthesize cDNA. Fluorescence real-time PCR was performed with TB GreenTM Premix Ex Taq II reagents (TaKaRa, Japan) on LightCycler96 Real-Time PCR System. For quantification, monocyte chemoattractant protein-1 (*Mcp-1*) and C–X–C motif chemokine ligand 1 (*Cxcl1*) mRNA levels were normalized to *Gapdh* mRNA level. The primer sequences are listed in Table 1.

Cell culture, transfection, and treatment

The mouse proximal tubular epithelial cell line BUMPT was initially received from Dr. Wilfred Lieberthal in Boston University and cultured as previously described [44]. Transfection and treatment in BUMPT cells were described as follows:

1. BUMPT cells were daily incubated with different concentrations (0, 0.5, 1, and 2 μM) of cisplatin for 7 h followed by incubation with cisplatin-free medium for another 17 h for 4 continuous days.

2. BUMPT cells were incubated with cisplatin (2 μM) or saline for 7 h daily for 4 days and then treated with 5 mM 4-PBA, 1 μM GSK2656157 or corresponding vehicle for 17 h starting from the last cisplatin treatment.

3. BUMPT cells were transfected with kinase-dead PKCδ (PKCδ-KD) plasmid or PC-DNA3.1b vector plasmid by Lipofectamine 3000. 24 h after transfection, the cells were then incubated with cisplatin (2 μM) or saline for 7 h daily for 4 days.

4. BUMPT cells were transfected with *Pkcδ*-shRNA or scrambled-shRNA with Lipofectamine 3000. 24 h after transfection, the cells were then incubated with or without cisplatin (2 μM) for 7 h daily for 4 days. These shRNAs were synthesized by Youbio Biological Technology Co., Ltd. (Changsha, China). The *Pkcδ* shRNA target sequence was as follows: 5`-GGAAGACACTGGTACAGAAGA-3`.

Table 1 Primer sequences used for quantitative real-time PCR

Gene	Primer sequences	
Cxcl1	Forward	5′-CTGGGATTCACCTCAAGA ACATC-3′
	Reverse	5′-CAGGGTCAAGGCAAGCCTC-3′
Mcp-1	Forward	5′-TAAAAACCTGGATCGGAA CCAAA-3′
	Reverse	5′-GCATTAGCTTCAGATTTACGGGT-3′
Gapdh	Forward	5′-AGGTCGGTGTGAACGGATTTG-3′
	Reverse	5′-GGGGTCGTTGATGGCAACA-3′

5. BUMPT cells were transfected with PKCδ active fragment (PKCδ-CF) plasmid or PC-DNA3.1b vector plasmid using Lipofectamine 3000. PKCδ-KD and PKCδ-CF plasmids were initially received from Jae-Won Soh at Inha University. 24 h after transfection, the cells were incubated with cisplatin (2 μM) or saline for 7 h daily for 4 days. After the last cisplatin treatment, the cells were treated with 1 μM GSK2656157 or the vehicle for another 17 h.

Phase contrast microscopy

BUMPT cells show a cobblestone morphology under normal physiological conditions, and change to a spindle-shaped, fibroblast-like morphology upon pro-fibrotic stimuli [34]. To evaluate cell morphological changes during RLDC treatment, phase contrast microscopy images of live cells were collected immediately after treatment using a LEICA DMI3000 B microscope.

Co-immunoprecipitation of PERK and PKCδ

BUMPT cells were lysed in ice-cold immunoprecipitation lysis buffer (150 mM NaCl, 5% glycerol, 50 mM Tris HCl pH 8.0, 1 mM $MgCl_2$, 1.0% NP40) with 1% protease inhibitor cocktail on ice for 30 min. After centrifugation at 12,000 rpm for 10 min at 4 °C, the supernatants were incubated with anti-PERK (1:150 dilution), anti-PKCδ antibody (1:100 dilution), or IgG (1:150 dilution) as control overnight at 4 °C, and the antigen–antibody complexes were then precipitated by the Protein A/G PLUS-Agarose. The immunoprecipitation complexes were washed, eluted, and then analyzed by immunoblot analysis.

Statistics

GraphPad Prism 7 was used for statistical analysis. Data were presented as means ± SDs. To analyze differences, the t-test was used between two groups, and the ANOVA was used for more than 2 groups. P values < 0.05 were regarded as significantly different.

Role of the funding source

The funders had no role in the design, analysis, and reporting of the study and the writing of this article.

Results

ER stress is induced in the kidneys of mice after RLDC treatment

To investigate the potential mechanism underlying cisplatin-induced CKD, RLDC treatment that recapitulates the clinical settings was performed to induce chronic kidney changes in mice (Supplementary Fig. 1a) [43]. Kidney functions of the mice were evaluated by measuring GFR, serum creatinine, and BUN. At 1 week (W) and 1 month (M) after RLDC treatment, GFR was dramatically decreased in mice, while serum creatinine and BUN were significantly increased compared to saline-treated mice (Supplementary Fig. 1b–d), suggesting that RLDC treatment caused chronic renal dysfunction. Histological analysis via HE staining showed that RLDC treatment caused dramatic structural changes in kidneys, including tubular dilation, cast formation, tubular necrosis, tubular atrophy, and inflammatory cell infiltration (Supplementary Fig. 1e). Quantification analysis showed a time-dependent increase of tubular atrophy after RLDC treatment (Supplementary Fig. 1f). Renal interstitial accumulation of collagen was markedly increased in a time-dependent manner after RLDC treatment, as shown by Masson trichrome staining (Supplementary Fig. 1 g, h). Collectively, these findings indicate the development of CKD after RLDC treatment in mice.

For ER stress, our immunoblot analysis demonstrated the increase of phosphorylated/activated PERK (p-PERK) and phosphorylated/activated eIF2α (p-eIF2α) (Supplementary Fig. 1i, j) in kidney tissues after RLDC treatment, indicating the activation of PERK-mediated UPR pathway. Immunohistochemical analysis also showed an increase in the signal intensity of p-PERK in renal tubules of RLDC-treated mice compared to saline control (Supplementary Fig. 1 k, l). Together, these results indicate that ER stress is activated in the kidneys during cisplatin-induced CKD.

Inhibition of ER stress attenuates renal dysfunction, tubular atrophy, kidney fibrosis, and inflammation in mice following RLDC treatment

To evaluate the function of ER stress in cisplatin-induced CKD, we assessed the effect of ER stress inhibition. After the last cisplatin injection, administration of 4-PBA and TUDCA significantly suppressed PERK and eIF2α phosphorylation in RLDC-treated mice in immunoblot analysis (Supplementary Fig. 2a–d) and immunohistochemical staining (Supplementary Fig. 2e, f).

Notably, both 4-PBA and TUDCA significantly restored GFR and reduced serum creatinine and BUN in RLDC-treated mice (Fig. 1a–c). RLDC treatment reduced kidney weight/body weight ratio, which was significantly alleviated by 4-PBA and TUDCA treatment (Fig. 1d). Moreover, following RLDC treatment, 4-PBA- or TUDCA-treated mice showed significantly less kidney tubular atrophy (Fig. 1e, f), lower levels of extracellular matrix proteins FN, vimentin, and α-SMA, and fewer accumulation of collagens (Fig. 1g–l) when compared to the mice with vehicle treatment. Collectively, these results demonstrate that inhibition of ER stress is protective against cisplatin-induced CKD.

Inflammation critically contributes to the development and progression of CKD [44–46]. We, thus, evaluated the effects of TUDCA and 4-PBA on renal inflammation in mice following RLDC treatment. Immunohistochemical staining of F4/80 indicated an occurrence of renal infiltration of macrophages in RLDC-treated mice, and the number of macrophages infiltrated into kidneys was significantly reduced by 4-PBA or TUDCA treatment in RLDC-treated mice (Fig. 2a, b). We further analyzed proinflammatory cytokine expression, including *Mcp-1* and *Cxcl1*, by quantitative reverse-transcriptase PCR. RLDC induced over 30-fold increases of both *Mcp-1* and *Cxcl1* in kidneys, which were significantly attenuated by 4-PBA and TUDCA (Fig. 2c, d), further supporting the beneficial effects of ER stress inhibitors.

ER stress is induced by RLDC treatment in renal proximal tubular BUMPT cells in vitro

We also examined ER stress in an in vitro cell model of cisplatin-induced CKD that was established in our recent study [43]. As shown in Supplementary Fig. 3a, the BUMPT cells subjected to repeated 2 μM cisplatin treatment displayed a spindle-shaped morphology, while the vehicle-treated cells maintained a "cobblestone" morphology. Immunoblot analysis also showed that repeated 2 μM cisplatin treatment dramatically increased FN, vimentin, p-PERK, and p-eIF2α expression (Supplementary Fig. 3b–e). These observations indicate that RLDC of 2 μM cisplatin induces the fibrotic changes and ER stress in BUMPT cells, recapitulating the essential findings of RLDC-treated mice.

Inhibition of ER stress reduces RLDC-induced fibrotic changes and inflammation in BUMPT cells

In vitro, we determined the function of ER stress in RLDC-induced fibrotic changes in BUMPT cells via administrating a single dose of 4-PBA after the last cisplatin treatment. As shown in Fig. 3a and b, 4-PBA attenuated RLDC-induced phosphorylation of both PERK and eIF2α in these cells. 4-PBA also markedly ameliorated RLDC-induced morphological changes (Fig. 3c) and FN, collagen I, Collagen IV, and vimentin expression (Fig. 3d, e). In addition, 4-PBA

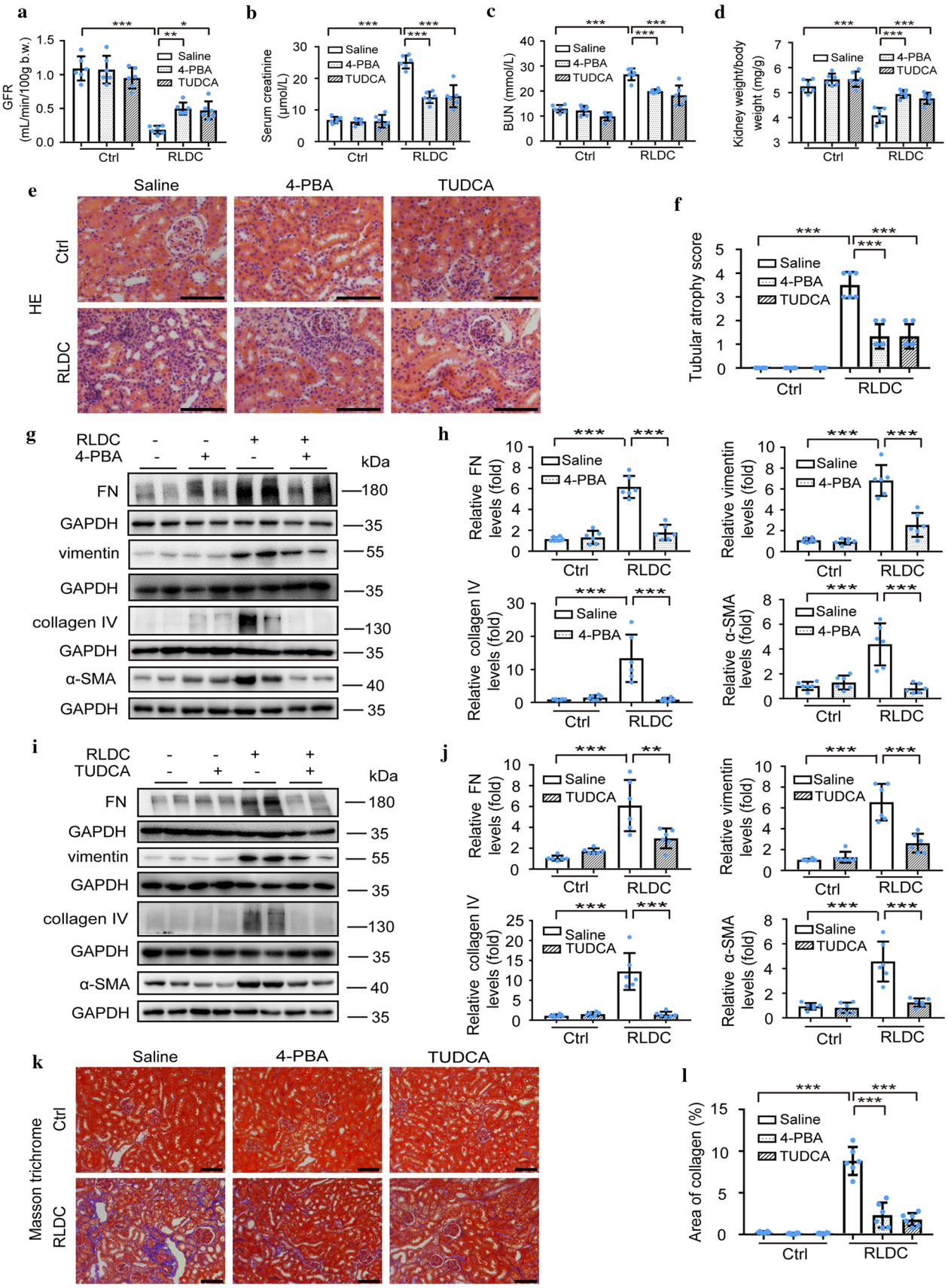
a
GFR (mL/min/100g b.w.)
Saline
4-PBA
TUDCA
Ctrl
RLDC
b
Serum creatinine (μmol/L)
c
BUN (mmol/L)
d
Kidney weight/body weight (mg/g)
e
Saline
4-PBA
TUDCA
HE
Ctrl
RLDC
f
Tubular atrophy score
g
RLDC
4-PBA
kDa
FN
GAPDH
vimentin
collagen IV
α-SMA
h
Relative FN levels (fold)
Relative vimentin levels (fold)
Relative collagen IV levels (fold)
Relative α-SMA levels (fold)
i
TUDCA
j
k
Masson trichrome
l
Area of collagen (%)

◂**Fig. 1** 4-PBA and TUDCA attenuate renal dysfunction, tubular atrophy, and kidney fibrosis in post-repeated low-dose cisplatin (RLDC) mouse kidneys. C57BL/6 male mice were subjected to four weekly injections of cisplatin (8 mg/kg). 4-PBA, TUDCA, or saline was given daily after the last injection of cisplatin for 1 week. FITC-Sinistrin was injected via tail vein before sacrifice to measure glomerular filtration rate (GFR). Blood and kidney tissues were collected 1 month after the last injection of cisplatin. **a** Quantitative analysis of GFR. **b** Concentration of serum creatinine. **c** Concentration of blood urea nitrogen (BUN). **d** Ratio of kidney weight to body weight. **e** Representative HE staining images. Bar = 100 μm. **f** Pathological tubular atrophy score. **g–j** Immunoblot analysis of FN, vimentin, collagen IV, α-SMA, and GAPDH. For quantification, the protein was analyzed through densitometry and then normalized with GAPDH. **k**, **l** Representative images of Masson trichrome staining and quantitative analysis. Bar = 100 μm. $N = 6$ mice. $^{*}p < 0.05$; $^{**}p < 0.01$; $^{***}p < 0.001$

suppressed RLDC-induced expression of *Mcp-1* and *Cxcl1* (Fig. 3f–g). Collectively, these findings indicate the role of ER stress in RLDC-induced fibrotic changes and inflammation in this cell culture model.

Inhibition of PERK alleviates RLDC-induced fibrotic changes and inflammation in BUMPT cells

Upon ER stress, the sensor proteins PERK, ATF6, and/or IRE1-mediated UPR are activated to reduce protein load and restore ER homeostasis [24]. RLDC induced a remarkable activation of the PERK–eIF2α pathway in kidney tubular cells both in vivo (Supplementary Fig. 1i–l) and in vitro (Supplementary Fig. 3d–e). We, therefore, performed further analysis to determine whether the PERK-mediated UPR pathway plays a major role in cisplatin-induced CKD. GSK2656157 is a specific PERK inhibitor that blocks PERK autophosphorylation through interacting with the PERK kinase domain [47]. Under the condition of RLDC treatment, GSK2656157 significantly attenuated RLDC-induced PERK phosphorylation (Fig. 4a, b), prevented RLDC-induced morphological changes (Fig. 4c), and alleviated RLDC-induced expression of FN, vimentin, and collagen IV in BUMPT cells (Fig. 4d, e). In addition, GSK2656157 suppressed the expression of *Mcp-1* and *Cxcl1* following RLDC treatment (Fig. 4f, g). Together, these results suggest that activation of PERK–eIF2α pathway contributes critically to RLDC-induced pro-fibrotic phenotype in renal tubular cells.

Inhibition of PERK suppresses RLDC-induced PKCδ activation, and PERK physically interacts with PKCδ

PKCδ plays an important role in acute nephrotoxicity of cisplatin [40], but its involvement in cisplatin-induced CKD was unknown. We detected an increase of PKCδ phosphorylation at Y311 in the kidneys of mice subjected to RLDC treatment compared to vehicle-treated mice (Fig. 5a–d), indicative of PKCδ activation [39]. Importantly, treatment with 4-PBA or TUDCA significantly attenuated RLDC-induced PKCδ phosphorylation (Fig. 5a–d). Moreover, inhibition of PERK with GSK2656157 dramatically attenuated PKCδ phosphorylation following RLDC treatment (Fig. 6a, b). In addition, co-immunoprecipitation analysis demonstrated that PERK co-immunoprecipitated PKCδ in BUMPT cells, and vice versa, suggesting that PERK physically interacts with PKCδ in these cells (Fig. 6c, d). Therefore, PERK may interact with PKCδ for its activation during RLDC treatment.

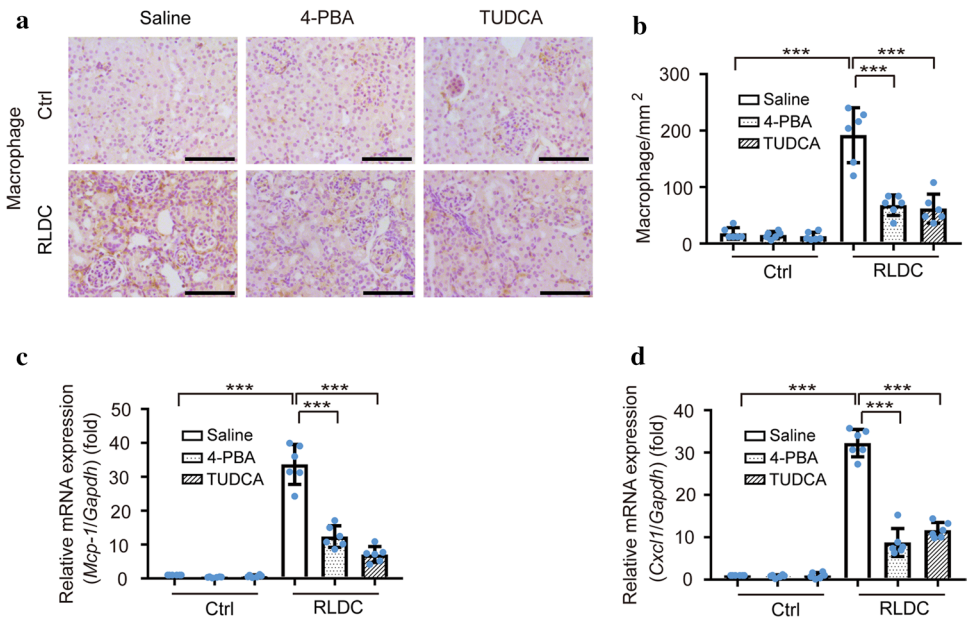

Fig. 2 4-PBA and TUDCA reduce kidney interstitial inflammation post-RLDC treatment in mouse kidneys. C57BL/6 male mice were subjected to four weekly injections of cisplatin (8 mg/kg). 4-PBA, TUDCA, or saline was given daily from the last injection of cisplatin for 1 week. Kidney tissues were collected 1 month after the last injection of cisplatin. **a**, **b** Representative immunohistochemical staining images and quantitative analysis of F4/80. Bar = 100 μm. **c**, **d** Quantitative real-time PCR analysis of *Mcp-1* and *Cxcl1* normalized with *Gapdh* as an internal control. $N = 6$ mice. $^{***}p < 0.001$

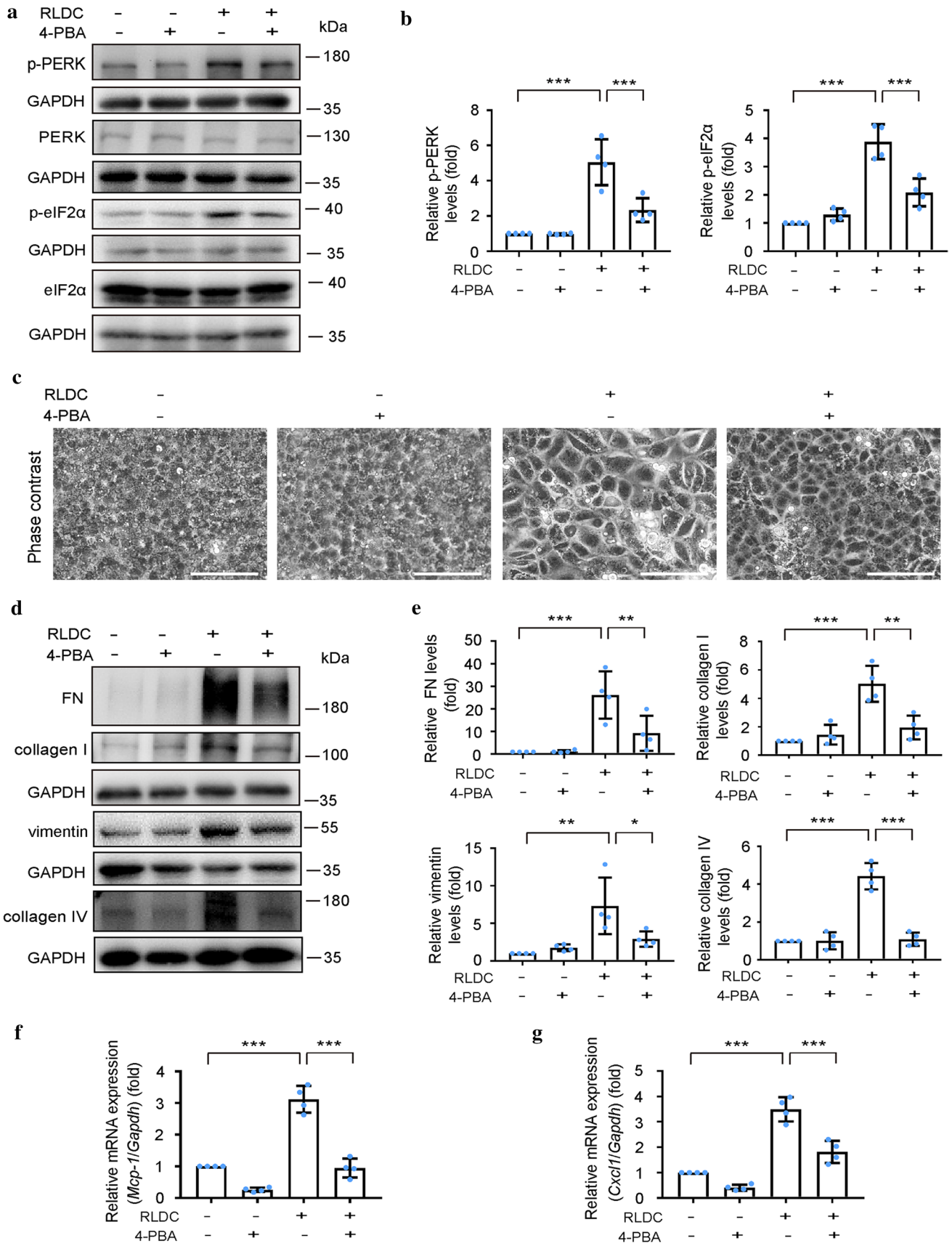
a
RLDC
4-PBA
kDa
p-PERK
GAPDH
PERK
GAPDH
p-eIF2α
GAPDH
eIF2α
GAPDH
180
35
130
35
40
35
40
35
b
Relative p-PERK levels (fold)
Relative p-eIF2α levels (fold)
***
c
Phase contrast
d
FN
collagen I
GAPDH
vimentin
GAPDH
collagen IV
GAPDH
180
100
35
55
35
180
35
e
Relative FN levels (fold)
Relative collagen I levels (fold)
Relative vimentin levels (fold)
Relative collagen IV levels (fold)
**
*
f
Relative mRNA expression (Mcp-1/Gapdh) (fold)
g
Relative mRNA expression (Cxcl1/Gapdh) (fold)

◂**Fig. 3** 4-PBA attenuates RLDC-induced fibrotic changes and cytokines production in cultured BUMPT cells. BUMPT cells were incubated with or without cisplatin (2 μM) for 7 h daily for 4 days and then treated with or without 5 mM 4-PBA for 17 h post last cisplatin treatment. **a**, **b** Immunoblot analysis of p-PERK, PERK, p-eIF2α, eIF2α, and GAPDH. For quantification, the protein was analyzed through densitometry and then normalized with GAPDH. **c** Representative images of phase contrast. Bar = 100 μm. **d**, **e** Immunoblot analysis of FN, collagen I, vimentin, collagen IV, and GAPDH. **f**, **g** Quantitative real-time PCR analysis of *Mcp-1* and *Cxcl1* with *Gapdh* as an internal control. $n = 4$. *$p < 0.05$; **$p < 0.01$; ***$p < 0.001$

PKCδ activation contributes to RLDC-induced pro-fibrotic and pro-inflammatory changes in BUMPT cells

We next determined whether PKCδ activation contributed to ER stress-induced fibrotic changes and inflammation following RLDC treatment. In BUMPT cells, overexpression of PKCδ-KD markedly attenuated RLDC-induced expression of FN, collagen IV, and vimentin (Fig. 7a, b) and significantly alleviated RLDC-induced expression of *Mcp-1* and *Cxcl1* (Fig. 7c, d). Consistently, silencing PKCδ with shRNA (Supplementary Fig. 4a and b) prevented RLDC-induced expression of FN, vimentin, and collagen IV in BUMPT cells (Fig. 7e, f). Moreover, the PERK inhibitor GSK2656157 suppressed RLDC-induced expression of FN and vimentin as well as pro-inflammatory cytokines *Mcp-1* and *Cxcl1*. Notably, these effects of GSK2656157 were reversed by the overexpression of PKCδ-CF (Fig. 7g–j). Collectively, these findings suggest that PKCδ acts downstream of PERK to contribute to RLDC-induced pro-fibrotic and pro-inflammatory changes in renal tubular cells.

Discussion

Cancer patients may develop chronic kidney problems or CKD after cisplatin-mediated chemotherapy, but the underlying mechanism remains largely unknown. In this research, we used both mice and cell models of RLDC treatment to demonstrate the involvement of ER stress and further elucidate the responsible PERK–PKCδ pathway. The main findings include: (1) RLDC-induced persistent ER stress in kidneys, characterized by the activation of PERK; (2) pharmacological inhibition of ER stress or PERK attenuated RLDC-induced CKD development in mice as well as the pro-fibrotic and pro-inflammatory changes in renal tubular cells; and (3) PKCδ was activated in an ER stress or PERK-dependent manner and acted downstream of PERK to mediate fibrotic changes in renal tubular cells. In addition, co-immunoprecipitation analysis also provided preliminary evidence for the physical interaction of PERK with PKCδ. Together, these results suggest that ER stress may contribute to the development of chronic kidney pathologies or CKD following cisplatin chemotherapy via the PERK–PKCδ pathway.

ER stress has been implicated as an important mechanism for the development of both AKI and CKD [32, 34, 35, 48, 49]. In addition, we have recently demonstrated that the persistence of ER stress facilitated the development of CKD post renal ischemic AKI [35]. In this study, we showed that ER stress was induced in kidney tubules following RLDC treatment (Supplementary Figs. 1i–l and 3d–e). More importantly, administration of ER stress inhibitor 4-PBA or TUDCA after the last cisplatin treatment dramatically attenuated RLDC-induced decline of both GFR and kidney weight/body weight ratio, and alleviated the increase of serum creatinine and BUN in mice as well as tubular atrophy and renal fibrosis even 1M after the RLDC treatment (Figs. 1 and 3c–e), suggesting that ER stress contributes critically to cisplatin-related CKD. Collectively, the findings from the present study and previous reports suggest that ER stress promotes the development of AKI and contributes to AKI–CKD transition.

Upon ER stress, the UPR pathways mediated by PERK, ATF6, and IRE1 are activated to restore ER homeostasis [24, 25]. In the present study, we showed that RLDC treatment dramatically increased the levels of phosphorylated PERK and phosphorylated eIF2α in mouse kidneys (Supplementary Fig. 1i–l) and renal tubular cells in vitro (Supplementary Fig. 3d–e), and notably, selective inhibition of PERK efficiently attenuated RLDC-induced fibrotic changes (Fig. 4c–e), suggesting that activation of PERK–eIF2α signaling pathway plays an important role in RLDC-induced CKD. Notably, ATF6- and IRE1-mediated signaling pathways have also been implicated in CKD [50, 51]. Further research is needed to investigate the involvement of ATF6- and IRE1-mediated UPR pathways in RLDC-induced CKD.

Short-term induction of PERK can promote cell survival through inducing eIF2α phosphorylation to arrest global protein translation, while prolonged PERK activation can trigger apoptosis [26]. How does PERK activation promote CKD? In the present study, we have provided several lines of evidence suggesting that PKCδ acts downstream of PERK. First, inhibition of ER stress or selective inhibition of PERK significantly suppressed RLDC-induced PKCδ activation in the kidneys of mice (Fig. 5) and in BUPMT cells in vitro (Fig. 6a–b). Second, PERK physically interacts with PKCδ (Fig. 6c–d). Third, suppression of PKCδ via overexpression of PKCδ-KD or *Pkcδ* shRNA dramatically alleviated RLDC-induced fibrotic changes in BUMPT cells in vitro (Fig. 7a, b, e, f). Finally, enhancement of PKCδ activity by overexpression of PKCδ-CF diminished the beneficial effect of PERK inhibition in RLDC-treated BUMPT cells (Fig. 7g, h).

PKCδ activation has been implicated in cisplatin-induced AKI [40, 41]. PKCδ inhibition not only protected kidneys

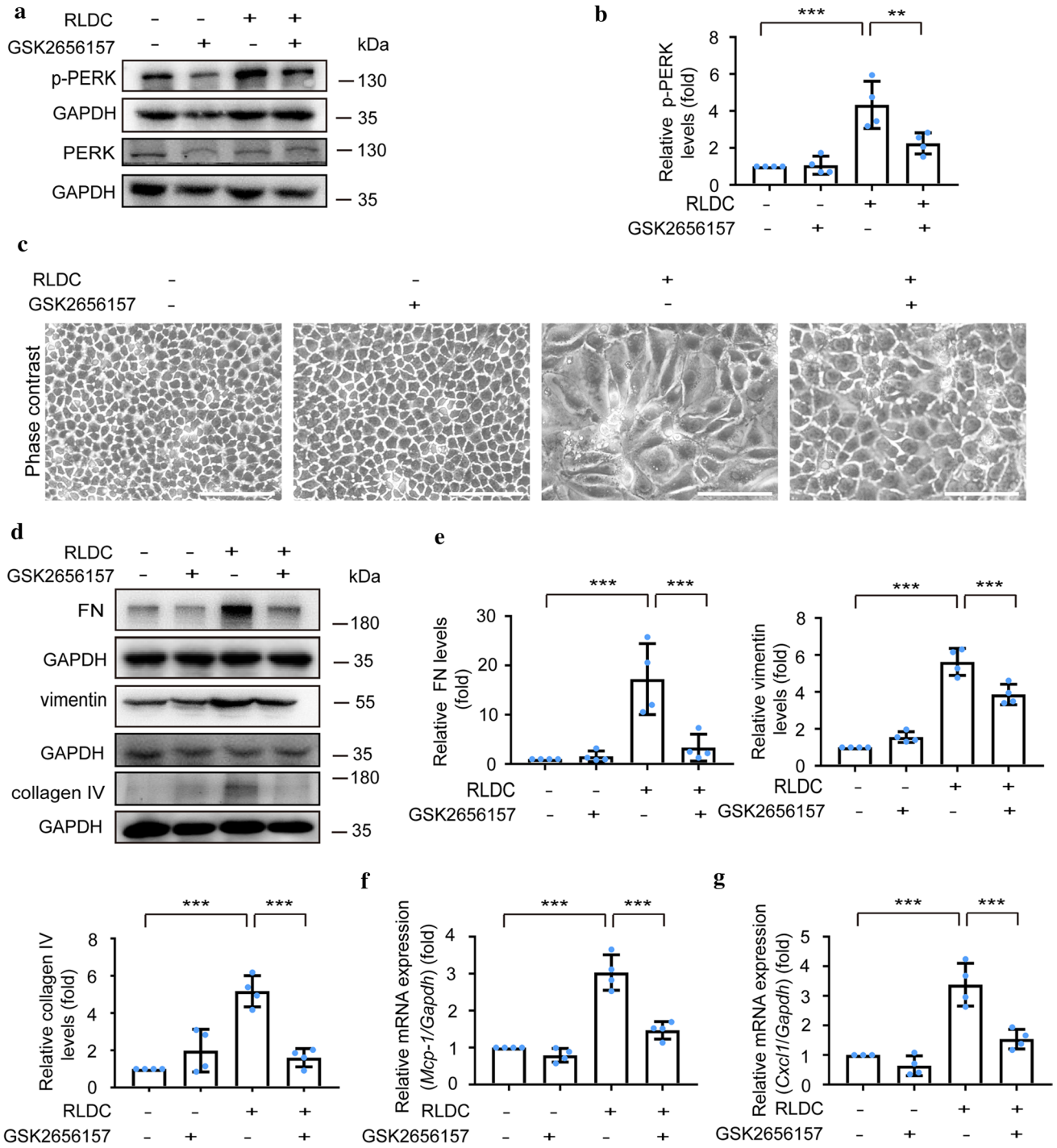

Fig. 4 GSK2656157 attenuates fibrotic changes and cytokines production in BUMPT cells following RLDC treatment. BUMPT cells were incubated with or without cisplatin (2 μM) for 7 h daily for 4 days and then treated with or without 1 μM GSK2656157 for 17 h post last cisplatin treatment. **a**, **b** Immunoblot analysis of p-PERK, PERK, and GAPDH. For quantification, the protein was analyzed through densitometry and then normalized with GAPDH. **c** Representative images of phase contrast. Bar = 100 μm. **d**, **e** Immunoblot analysis of FN, vimentin, collagen IV, and GAPDH. **f**, **g** Quantitative real-time PCR analysis of *Mcp-1* and *Cxcl1* with *Gapdh* as an internal control. $n = 4$. $^{**}p < 0.01$; $^{***}p < 0.001$

from cisplatin-induced AKI but also preserved or even enhanced the chemotherapeutic effects of cisplatin among several mice tumor models [40]. PKCδ activation has been implicated in promoting liver fibrosis [52] and right ventricular fibrosis [53], but it may attenuate bleomycin-induced pulmonary fibrosis [54]. The role of PKCδ in renal fibrosis

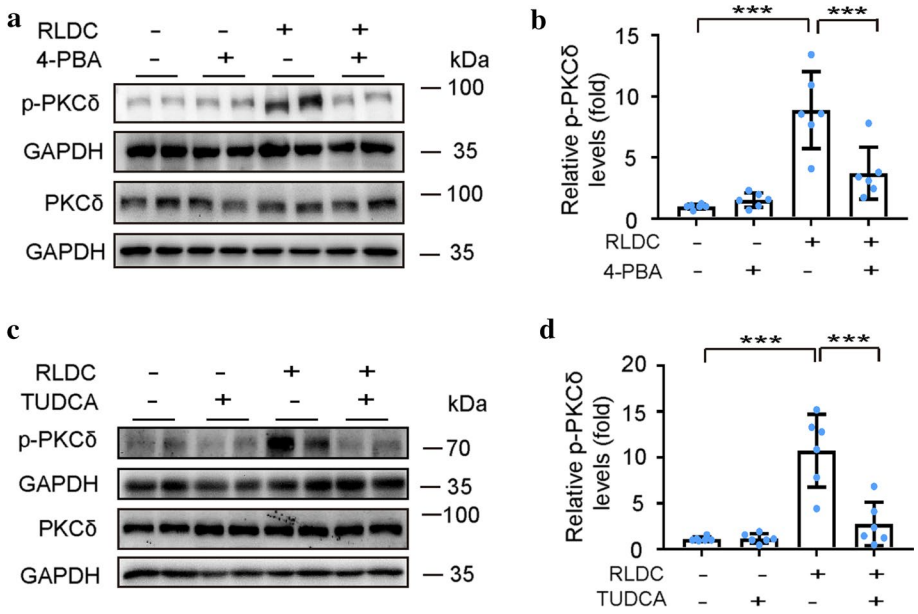

Fig. 5 4-PBA and TUDCA suppress RLDC-induced PKCδ activation in mouse kidneys. C57BL/6 male mice were subjected to four weekly injections of cisplatin (8 mg/kg). 4-PBA, TUDCA, or saline was given daily from the last injection of cisplatin for 1 week. Kidney tissues were collected 1 month after the last injection of cisplatin. **a**–**d** Immunoblot analysis of p-PKCδ, PKCδ, and GAPDH. For quantification, the protein was analyzed through densitometry and then normalized with GAPDH. $N=6$ mice. ***$p<0.001$

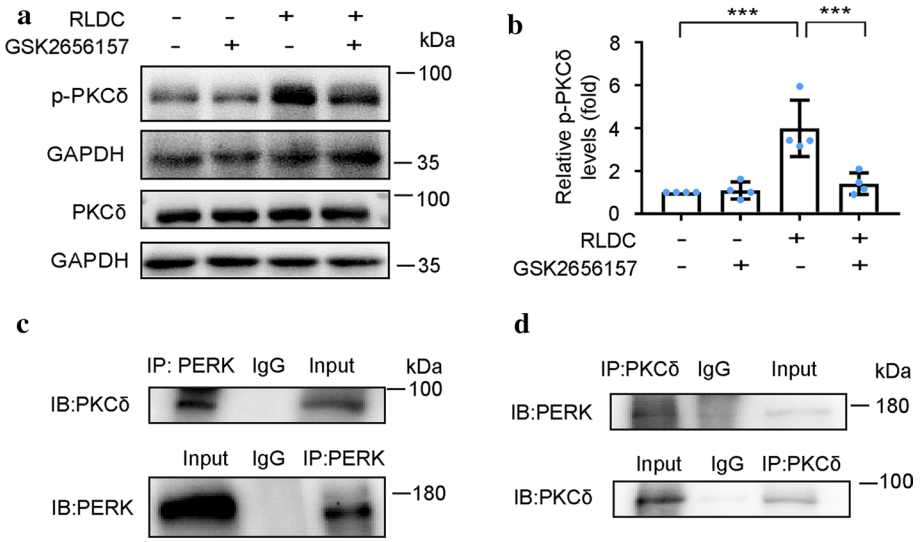

Fig. 6 Role of PERK in PKCδ activation in RLDC-treated BUMPT cells: effect of GSK2656157 and co-immunoprecipitation analysis. BUMPT cells were incubated with or without cisplatin (2 μM) for 7 h daily for 4 days and then treated with or without 1 μM GSK2656157 for 17 h post last cisplatin treatment (**a**, **b**). BUMPT cells were incubated with cisplatin (2 μM) for 7 h daily for 4 days (**c**, **d**). **a**, **b** Immunoblot analysis of p-PKCδ, PKCδ, and GAPDH. For quantification, the protein was analyzed through densitometry and then normalized with GAPDH. **c**, **d** Reciprocal co-immunoprecipitation of endogenous PERK and PKCδ. $n=4$. ***$p<0.001$

remains unknown. In this study, we showed that suppression of PKCδ via overexpression of PKCδ-KD or *Pkcδ* shRNA dramatically alleviated RLDC-induced fibrotic changes in BUMPT cells (Fig. 7a, b, e, f), suggesting a pro-fibrotic role of PKCδ during RLDC-induced renal fibrosis and CKD. However, the function of PKCδ in this pathological condition remains to be verified in vivo.

Maladaptive repair after initial kidney injury promotes the development of chronic kidney pathologies and CKD [55–58]. Inflammation has been implicated as an important mechanism for maladaptive kidney repair after AKI [59]. In the present study, we showed that RLDC treatment induced the infiltration of macrophages and the expression of pro-inflammatory cytokines, including *Mcp-1* and *Cxcl1*, which were dramatically suppressed by ER stress or PERK inhibitors (Figs. 2, 3f–g, 4f–g), suggesting a pro-inflammatory role of ER stress during RLDC-induced CKD. Notably, the effect of the PERK inhibitor was abrogated by

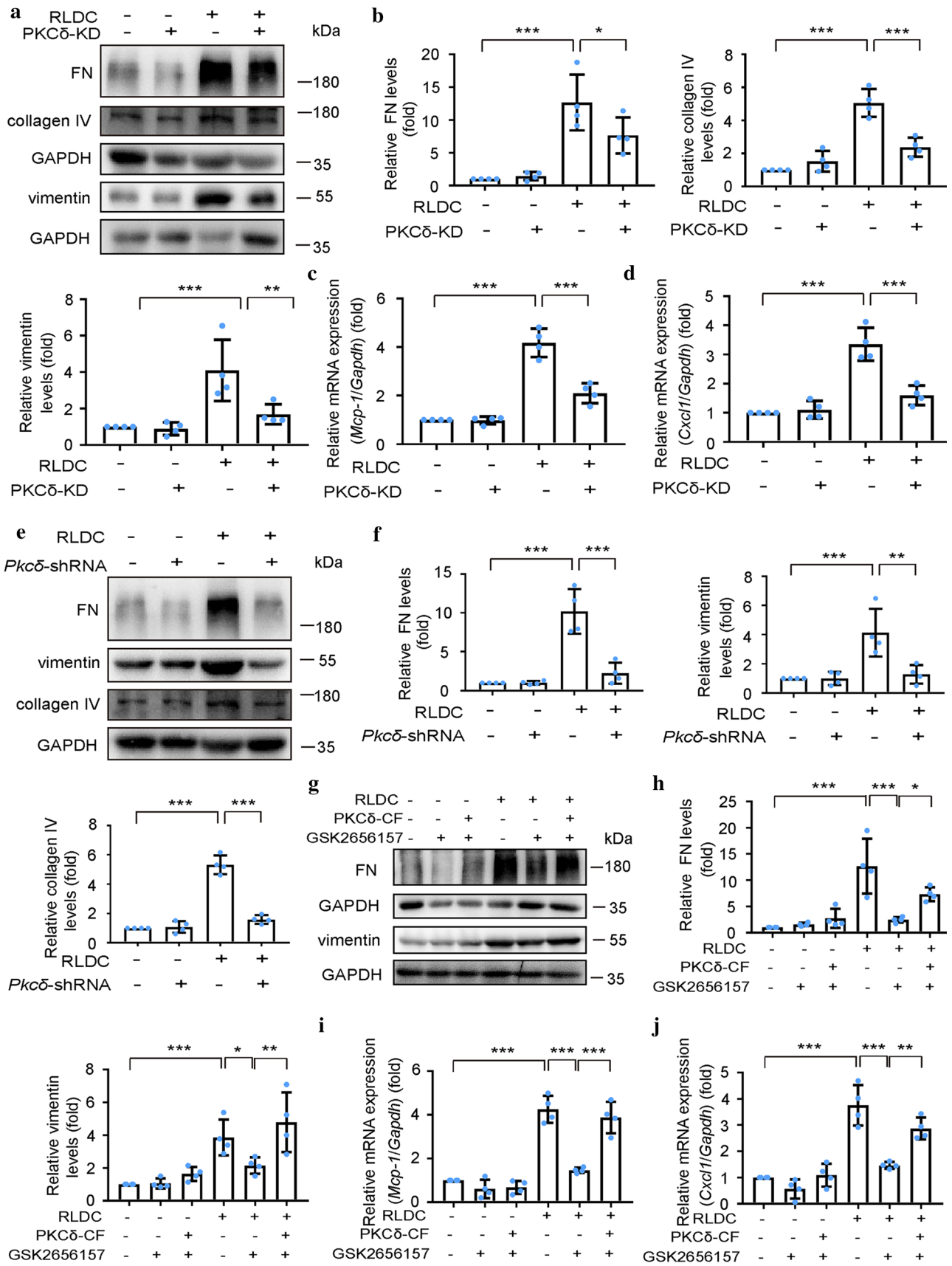
a
RLDC
PKCδ-KD
kDa
FN
collagen IV
GAPDH
vimentin
GAPDH
180
180
35
55
35
b
Relative FN levels (fold)
Relative collagen IV levels (fold)
c
Relative vimentin levels (fold)
Relative mRNA expression (Mcp-1/Gapdh) (fold)
d
Relative mRNA expression (Cxcl1/Gapdh) (fold)
e
Pkcδ-shRNA
f
g
PKCδ-CF
GSK2656157
h
i
j

◂**Fig. 7** PKCδ contributes to RLDC-induced fibrotic changes and inflammation in BUMPT cells. BUMPT cells were transfected with PKCδ-KD or PC-DNA3.1b vector, and then incubated with or without cisplatin (2 μM) for 7 h daily for 4 days (**a**–**d**). Or BUMPT cells were transfected with or without *Pkcδ*-shRNA, and then incubated with or without 2 μM cisplatin for 7 h daily for 4 days (**e**–**f**). Or BUMPT cells were transfected with or without PKCδ-CF, and then incubated with or without cisplatin (2 μM) for 7 h daily for 4 days followed by treatment with or without 1 μM GSK2656157 for 17 h post last cisplatin treatment (**g**–**j**). **a**, **b**, **e**–**h** Immunoblot analysis of FN, collagen IV, vimentin, and GAPDH. For quantification, the protein was analyzed through densitometry and then normalized with GAPDH. **c**, **d**, **i**, **j** Quantitative real-time PCR analysis of *Mcp-1*, *Cxcl1,* and *Gapdh* (internal control). $n=4$. $^{*}p<0.05$; $^{**}p<0.01$; $^{***}p<0.001$

the enhancement of PKCδ activity through overexpression of PKCδ-CF (Fig. 7i–j), suggesting that PKCδ activation, at least partially, contributes to the inflammatory response during RLDC-induced CKD. PERK–eIF2α-mediated signaling pathway may activate NF-κB, a transcription factor that plays a vital role in inflammation [29–31]. PKCδ has also been implicated in NF-κB-mediated inflammatory response [52, 60, 61]. Recent research demonstrated that NF-κB involved in cisplatin-induced AKI [62–66]. The role of NF-κB-mediated inflammation in RLDC-induced CKD remains to be confirmed. Besides inflammation, cell senescence, cell cycle arrest at the G2/M phase, and persistent autophagy are also important mechanisms of maladaptive repair after AKI [44, 56, 57, 67]. The involvement of these mechanisms and their connections with ER stress signaling in RLDC-induced CKD remains to be investigated.

In conclusion, this research offers both in vivo and in vitro evidence that persistent ER stress contributes critically to RLDC-induced CKD. Mechanistically, we show that PERK-mediated UPR signaling pathway plays a critical role in this pathological condition. Moreover, we provide further evidence that PERK may physically interact with PKCδ and induce fibrotic changes and inflammation in renal tubular cells by activating PKCδ. Together, these results demonstrate that ER stress-induced activation of the PERK–PKCδ pathway contributes critically to cisplatin-induced CKD, suggesting that this pathway may be an effective therapeutic target for chronic cisplatin nephrotoxicity in cancer patients.

Supplementary Information The online version contains supplementary material available at https://doi.org/10.1007/s00018-022-04480-2.

Acknowledgements The authors would like to thank Huadong Medicine Co., Ltd (Hangzhou, China) for providing technical support of transcutaneous measurement of GFR in this study.

Author contributions ZD, SS, and CT designed the study. SS and HW did most of the experiments. ZD, SS, HW, and CT performed data analysis. All authors contributed to the preparation, writing, and final approval of the manuscript.

Funding This study was financially supported by the National Key R&D Program of China [2020YFC2005004] and the National Natural Science Foundation of China [81720108008, 81870474].

Data availability All data supporting the findings during this study are available in this manuscript and supplementary files.

Declarations

Conflict of interest All authors declared no competing interests.

Ethics approval All animal experiments were performed following the protocol approved by the Animal Ethics Committee of The Second Xiangya Hospital of Central South University with the Approval number 2020076.

Ethics approval and consent to participate Not applicable.

Consent for publication Not applicable.

References

1. Cao W, Yuan Y, Liu X, Li Q, An X, Huang Z, Wu L, Zhang B, Zhang A, Xing C (2019) Adenosine kinase inhibition protects against cisplatin-induced nephrotoxicity. Am J Physiol Renal Physiol 317(1):F107–F115. https://doi.org/10.1152/ajprenal.00385.2018
2. Cao X, Nie X, Xiong S, Cao L, Wu Z, Moore PK, Bian JS (2018) Renal protective effect of polysulfide in cisplatin-induced nephrotoxicity. Redox Biol 15:513–521. https://doi.org/10.1016/j.redox.2018.01.012
3. Deng B, Lin Y, Ma S, Zheng Y, Yang X, Li B, Yu W, Xu Q, Liu T, Hao C, He R, Ding F (2017) The leukotriene B4-leukotriene B4 receptor axis promotes cisplatin-induced acute kidney injury by modulating neutrophil recruitment. Kidney Int 92(1):89–100. https://doi.org/10.1016/j.kint.2017.01.009
4. Galgamuwa R, Hardy K, Dahlstrom JE, Blackburn AC, Wium E, Rooke M, Cappello JY, Tummala P, Patel HR, Chuah A, Tian L, McMorrow L, Board PG, Theodoratos A (2016) Dichloroacetate prevents cisplatin-induced nephrotoxicity without compromising cisplatin anticancer properties. J Am Soc Nephrol 27(11):3331–3344. https://doi.org/10.1681/ASN.2015070827
5. Gu X, Yang H, Sheng X, Ko YA, Qiu C, Park J, Huang S, Kember R, Judy RL, Park J, Damrauer SM, Nadkarni G, Loos RJF, My VTH, Chaudhary K, Bottinger EP, Paranjpe I, Saha A, Brown C, Akilesh S, Hung AM, Palmer M, Baras A, Overton JD, Reid J, Ritchie M, Rader DJ, Susztak K (2021) Kidney disease genetic risk variants alter lysosomal beta-mannosidase (MANBA) expression and disease severity. Sci Transl Med. https://doi.org/10.1126/scitranslmed.aaz1458
6. Humanes B, Camano S, Lara JM, Sabbisetti V, Gonzalez-Nicolas MA, Bonventre JV, Tejedor A, Lazaro A (2017) Cisplatin-induced renal inflammation is ameliorated by cilastatin nephroprotection. Nephrol Dial Transplant 32(10):1645–1655. https://doi.org/10.1093/ndt/gfx005
7. Jung YJ, Park W, Kang KP, Kim W (2020) SIRT2 is involved in cisplatin-induced acute kidney injury through regulation of mitogen-activated protein kinase phosphatase-1. Nephrol Dial Transplant 35(7):1145–1156. https://doi.org/10.1093/ndt/gfaa042
8. Kumar G, Solanki MH, Xue X, Mintz R, Madankumar S, Chatterjee PK, Metz CN (2017) Magnesium improves cisplatin-mediated

tumor killing while protecting against cisplatin-induced nephrotoxicity. Am J Physiol Renal Physiol 313(2):F339–F350. https://doi.org/10.1152/ajprenal.00688.2016
9. Li Z, Xu K, Zhang N, Amador G, Wang Y, Zhao S, Li L, Qiu Y, Wang Z (2018) Overexpressed SIRT6 attenuates cisplatin-induced acute kidney injury by inhibiting ERK1/2 signaling. Kidney Int 93(4):881–892. https://doi.org/10.1016/j.kint.2017.10.021
10. Liu M, Grigoryev DN, Crow MT, Haas M, Yamamoto M, Reddy SP, Rabb H (2009) Transcription factor Nrf2 is protective during ischemic and nephrotoxic acute kidney injury in mice. Kidney Int 76(3):277–285. https://doi.org/10.1038/ki.2009.157
11. Oh CJ, Ha CM, Choi YK, Park S, Choe MS, Jeoung NH, Huh YH, Kim HJ, Kweon HS, Lee JM, Lee SJ, Jeon JH, Harris RA, Park KG, Lee IK (2017) Pyruvate dehydrogenase kinase 4 deficiency attenuates cisplatin-induced acute kidney injury. Kidney Int 91(4):880–895. https://doi.org/10.1016/j.kint.2016.10.011
12. Zhang J, Rudemiller NP, Patel MB, Wei Q, Karlovich NS, Jeffs AD, Wu M, Sparks MA, Privratsky JR, Herrera M, Gurley SB, Nedospasov SA, Crowley SD (2016) Competing actions of type 1 Angiotensin II receptors expressed on T lymphocytes and kidney epithelium during cisplatin-induced AKI. J Am Soc Nephrol 27(8):2257–2264. https://doi.org/10.1681/ASN.2015060683
13. Zhang J, Zhao T, Wang C, Meng Q, Huo X, Wang C, Sun P, Sun H, Ma X, Wu J, Liu K (2021) Catalpol-induced AMPK activation alleviates cisplatin-induced nephrotoxicity through the mitochondrial-dependent pathway without compromising its anticancer properties. Oxid Med Cell Longev 2021:7467156. https://doi.org/10.1155/2021/7467156
14. Zhou J, An C, Jin X, Hu Z, Safirstein RL, Wang Y (2020) TAK1 deficiency attenuates cisplatin-induced acute kidney injury. Am J Physiol Renal Physiol 318(1):F209–F215. https://doi.org/10.1152/ajprenal.00516.2019
15. Burns CV, Edwin SB, Szpunar S, Forman J (2021) Cisplatin-induced nephrotoxicity in an outpatient setting. Pharmacotherapy 41(2):184–190. https://doi.org/10.1002/phar.2500
16. Latcha S, Jaimes EA, Patil S, Glezerman IG, Mehta S, Flombaum CD (2016) Long-term renal outcomes after cisplatin treatment. Clin J Am Soc Nephrol 11(7):1173–1179. https://doi.org/10.2215/CJN.08070715
17. Skinner R, Parry A, Price L, Cole M, Craft AW, Pearson AD (2009) Persistent nephrotoxicity during 10-year follow-up after cisplatin or carboplatin treatment in childhood: relevance of age and dose as risk factors. Eur J Cancer 45(18):3213–3219. https://doi.org/10.1016/j.ejca.2009.06.032
18. Black LM, Lever JM, Traylor AM, Chen B, Yang Z, Esman SK, Jiang Y, Cutter GR, Boddu R, George JF, Agarwal A (2018) Divergent effects of AKI to CKD models on inflammation and fibrosis. Am J Physiol Renal Physiol 315(4):F1107–F1118. https://doi.org/10.1152/ajprenal.00179.2018
19. Katagiri D, Hamasaki Y, Doi K, Negishi K, Sugaya T, Nangaku M, Noiri E (2016) Interstitial renal fibrosis due to multiple cisplatin treatments is ameliorated by semicarbazide-sensitive amine oxidase inhibition. Kidney Int 89(2):374–385. https://doi.org/10.1038/ki.2015.327
20. Li S, Lin Q, Shao X, Mou S, Gu L, Wang L, Zhang Z, Shen J, Zhou Y, Qi C, Jin H, Pang H, Ni Z (2019) NLRP3 inflammasome inhibition attenuates cisplatin-induced renal fibrosis by decreasing oxidative stress and inflammation. Exp Cell Res 383(1):111488. https://doi.org/10.1016/j.yexcr.2019.07.001
21. Sharp CN, Doll MA, Megyesi J, Oropilla GB, Beverly LJ, Siskind LJ (2018) Subclinical kidney injury induced by repeated cisplatin administration results in progressive chronic kidney disease. Am J Physiol Renal Physiol 315(1):F161–F172. https://doi.org/10.1152/ajprenal.00636.2017
22. Arga M, Oguz A, Pinarli FG, Karadeniz C, Citak EC, Emeksiz HC, Duran EA, Soylemezoglu O (2015) Risk factors for cisplatin-induced long-term nephrotoxicity in pediatric cancer survivors. Pediatr Int 57(3):406–413. https://doi.org/10.1111/ped.12542
23. Green DM, Wang M, Krasin M, Srivastava D, Onder S, Jay DW, Ness KK, Greene W, Lanctot JQ, Shelton KC, Zhu L, Mulrooney DA, Ehrhardt MJ, Davidoff AM, Robison LL, Hudson MM (2021) Kidney function after treatment for childhood cancer: a report from the St. Jude Lifetime Cohort Study. J Am Soc Nephrol. https://doi.org/10.1681/ASN.2020060849
24. Kaufman RJ (2002) Orchestrating the unfolded protein response in health and disease. J Clin Invest 110(10):1389–1398. https://doi.org/10.1172/JCI16886
25. Marciniak SJ, Chambers JE, Ron D (2021) Pharmacological targeting of endoplasmic reticulum stress in disease. Nat Rev Drug Discov. https://doi.org/10.1038/s41573-021-00320-3
26. Szegezdi E, Logue SE, Gorman AM, Samali A (2006) Mediators of endoplasmic reticulum stress-induced apoptosis. EMBO Rep 7(9):880–885. https://doi.org/10.1038/sj.embor.7400779
27. Charbonneau ME, O'Riordan MXD (2020) Reducing stress PERKs up anti-tumor immunity. Immunity 52(4):575–577. https://doi.org/10.1016/j.immuni.2020.03.012
28. Cunha DA, Cito M, Carlsson PO, Vanderwinden JM, Molkentin JD, Bugliani M, Marchetti P, Eizirik DL, Cnop M (2016) Thrombospondin 1 protects pancreatic beta-cells from lipotoxicity via the PERK-NRF2 pathway. Cell Death Differ 23(12):1995–2006. https://doi.org/10.1038/cdd.2016.89
29. Lei Z, Yue Y, Stone S, Wu S, Lin W (2020) NF-kappaB activation accounts for the cytoprotective effects of PERK activation on oligodendrocytes during EAE. J Neurosci 40(33):6444–6456. https://doi.org/10.1523/JNEUROSCI.1156-20.2020
30. Li W, Zhou X, Cai J, Zhao F, Cao T, Ning L, Luo C, Xiao X, Liu S (2021) Recombinant Treponema pallidum protein Tp0768 promotes proinflammatory cytokine secretion of macrophages through ER stress and ROS/NF-kappaB pathway. Appl Microbiol Biotechnol 105(1):353–366. https://doi.org/10.1007/s00253-020-11018-8
31. Qiao Q, Sun C, Han C, Han N, Zhang M, Li G (2017) Endoplasmic reticulum stress pathway PERK-eIF2alpha confers radioresistance in oropharyngeal carcinoma by activating NF-kappaB. Cancer Sci 108(7):1421–1431. https://doi.org/10.1111/cas.13260
32. Fan Y, Xiao W, Lee K, Salem F, Wen J, He L, Zhang J, Fei Y, Cheng D, Bao H, Liu Y, Lin F, Jiang G, Guo Z, Wang N, He JC (2017) Inhibition of reticulon-1A-mediated endoplasmic reticulum stress in early AKI attenuates renal fibrosis development. J Am Soc Nephrol 28(7):2007–2021. https://doi.org/10.1681/asn.2016091001
33. Inagi R, Ishimoto Y, Nangaku M (2014) Proteostasis in endoplasmic reticulum–new mechanisms in kidney disease. Nat Rev Nephrol 10(7):369–378. https://doi.org/10.1038/nrneph.2014.67
34. Shu S, Wang H, Zhu J, Liu Z, Yang D, Wu W, Cai J, Chen A, Tang C, Dong Z (2021) Reciprocal regulation between ER stress and autophagy in renal tubular fibrosis and apoptosis. Cell Death Dis 12(11):1016. https://doi.org/10.1038/s41419-021-04274-7
35. Shu S, Zhu J, Liu Z, Tang C, Cai J, Dong Z (2018) Endoplasmic reticulum stress is activated in post-ischemic kidneys to promote chronic kidney disease. EBioMedicine 37:269–280. https://doi.org/10.1016/j.ebiom.2018.10.006
36. Wei XM, Jiang S, Li SS, Sun YS, Wang SH, Liu WC, Wang Z, Wang YP, Zhang R, Li W (2021) Endoplasmic reticulum stress-activated PERK-eIF2alpha-ATF4 signaling pathway is involved in the ameliorative effects of ginseng polysaccharides against cisplatin-induced nephrotoxicity in mice. ACS Omega 6(13):8958–8966. https://doi.org/10.1021/acsomega.0c06339
37. Qvit N, Mochly-Rosen D (2014) The many hats of protein kinase C delta: one enzyme with many functions. Biochem Soc Trans 42(6):1529–1533. https://doi.org/10.1042/BST20140189

38. Greene MW, Ruhoff MS, Burrington CM, Garofalo RS, Orena SJ (2010) TNFalpha activation of PKCdelta, mediated by NFkappaB and ER stress, cross-talks with the insulin signaling cascade. Cell Signal 22(2):274–284. https://doi.org/10.1016/j.cellsig.2009.09.029
39. Steinberg SF (2008) Structural basis of protein kinase C isoform function. Physiol Rev 88(4):1341–1378. https://doi.org/10.1152/physrev.00034.2007
40. Pabla N, Dong G, Jiang M, Huang S, Kumar MV, Messing RO, Dong Z (2011) Inhibition of PKCdelta reduces cisplatin-induced nephrotoxicity without blocking chemotherapeutic efficacy in mouse models of cancer. J Clin Invest 121(7):2709–2722. https://doi.org/10.1172/JCI45586
41. Zhang D, Pan J, Xiang X, Liu Y, Dong G, Livingston MJ, Chen JK, Yin XM, Dong Z (2017) Protein kinase cdelta suppresses autophagy to induce kidney cell apoptosis in cisplatin nephrotoxicity. J Am Soc Nephrol 28(4):1131–1144. https://doi.org/10.1681/ASN.2016030337
42. Zheng M, Cai J, Liu Z, Shu S, Wang Y, Tang C, Dong Z (2019) Nicotinamide reduces renal interstitial fibrosis by suppressing tubular injury and inflammation. J Cell Mol Med 23(6):3995–4004. https://doi.org/10.1111/jcmm.14285
43. Fu Y, Cai J, Li F, Liu Z, Shu S, Wang Y, Liu Y, Tang C, Dong Z (2019) Chronic effects of repeated low-dose cisplatin treatment in mouse kidneys and renal tubular cells. Am J Physiol Renal Physiol 317(6):F1582–F1592. https://doi.org/10.1152/ajprenal.00385.2019
44. Livingston MJ, Ding HF, Huang S, Hill JA, Yin XM, Dong Z (2016) Persistent activation of autophagy in kidney tubular cells promotes renal interstitial fibrosis during unilateral ureteral obstruction. Autophagy 12(6):976–998. https://doi.org/10.1080/15548627.2016.1166317
45. Liu Y (2011) Cellular and molecular mechanisms of renal fibrosis. Nat Rev Nephrol 7(12):684–696. https://doi.org/10.1038/nrneph.2011.149
46. Rabb H, Griffin MD, McKay DB, Swaminathan S, Pickkers P, Rosner MH, Kellum JA, Ronco C, Acute Dialysis Quality Initiative Consensus XWG (2016) Inflammation in AKI: current understanding, key questions, and knowledge gaps. J Am Soc Nephrol 27(2):371–379. https://doi.org/10.1681/ASN.2015030261
47. Atkins C, Liu Q, Minthorn E, Zhang SY, Figueroa DJ, Moss K, Stanley TB, Sanders B, Goetz A, Gaul N, Choudhry AE, Alsaid H, Jucker BM, Axten JM, Kumar R (2013) Characterization of a novel PERK kinase inhibitor with antitumor and antiangiogenic activity. Cancer Res 73(6):1993–2002. https://doi.org/10.1158/0008-5472.CAN-12-3109
48. Ferre S, Deng Y, Huen SC, Lu CY, Scherer PE, Igarashi P, Moe OW (2019) Renal tubular cell spliced X-box binding protein 1 (Xbp1s) has a unique role in sepsis-induced acute kidney injury and inflammation. Kidney Int 96(6):1359–1373. https://doi.org/10.1016/j.kint.2019.06.023
49. Liu H, Baliga R (2005) Endoplasmic reticulum stress-associated caspase 12 mediates cisplatin-induced LLC-PK1 cell apoptosis. J Am Soc Nephrol 16(7):1985–1992. https://doi.org/10.1681/ASN.2004090768
50. Carlisle RE, Mohammed-Ali Z, Lu C, Yousof T, Tat V, Nademi S, MacDonald ME, Austin RC, Dickhout JG (2021) TDAG51 induces renal interstitial fibrosis through modulation of TGF-beta receptor 1 in chronic kidney disease. Cell Death Dis 12(10):921. https://doi.org/10.1038/s41419-021-04197-3
51. Chen YT, Jhao PY, Hung CT, Wu YF, Lin SJ, Chiang WC, Lin SL, Yang KC (2021) Endoplasmic reticulum protein TXNDC5 promotes renal fibrosis by enforcing TGF-beta signaling in kidney fibroblasts. J Clin Invest. https://doi.org/10.1172/JCI143645
52. Lee SJ, Kim SJ, Lee HS, Kwon OS (2019) PKCdelta mediates NF-kappaB inflammatory response and downregulates SIRT1 expression in liver fibrosis. Int J Mol Sci. https://doi.org/10.3390/ijms20184607
53. Chichger H, Vang A, O'Connell KA, Zhang P, Mende U, Harrington EO, Choudhary G (2015) PKC delta and betaII regulate angiotensin II-mediated fibrosis through p38: a mechanism of RV fibrosis in pulmonary hypertension. Am J Physiol Lung Cell Mol Physiol 308(8):L827–L836. https://doi.org/10.1152/ajplung.00184.2014
54. Wang J, Sun L, Nie Y, Duan S, Zhang T, Wang W, Ye RD, Hou S, Qian F (2020) Protein kinase C delta (PKCdelta) attenuates bleomycin induced pulmonary fibrosis via inhibiting NF-kappaB signaling pathway. Front Physiol 11:367. https://doi.org/10.3389/fphys.2020.00367
55. Basile DP, Bonventre JV, Mehta R, Nangaku M, Unwin R, Rosner MH, Kellum JA, Ronco C, Group AXW (2016) Progression after AKI: understanding maladaptive repair processes to predict and identify therapeutic treatments. J Am Soc Nephrol 27(3):687–697. https://doi.org/10.1681/ASN.2015030309
56. Canaud G, Brooks CR, Kishi S, Taguchi K, Nishimura K, Magassa S, Scott A, Hsiao LL, Ichimura T, Terzi F, Yang L, Bonventre JV (2019) Cyclin G1 and TASCC regulate kidney epithelial cell G2-M arrest and fibrotic maladaptive repair. Sci Transl Med. https://doi.org/10.1126/scitranslmed.aav4754
57. Ferenbach DA, Bonventre JV (2015) Mechanisms of maladaptive repair after AKI leading to accelerated kidney ageing and CKD. Nat Rev Nephrol 11(5):264–276. https://doi.org/10.1038/nrneph.2015.3
58. Tang C, Ma Z, Zhu J, Liu Z, Liu Y, Liu Y, Cai J, Dong Z (2019) P53 in kidney injury and repair: mechanism and therapeutic potentials. Pharmacol Ther 195:5–12. https://doi.org/10.1016/j.pharmthera.2018.10.013
59. Zheng Z, Li C, Shao G, Li J, Xu K, Zhao Z, Zhang Z, Liu J, Wu H (2021) Hippo-YAP/MCP-1 mediated tubular maladaptive repair promote inflammation in renal failed recovery after ischemic AKI. Cell Death Dis 12(8):754. https://doi.org/10.1038/s41419-021-04041-8
60. Njau F, Haller H (2021) Calcium dobesilate modulates PKCdelta-NADPH oxidase- MAPK-NF-kappaB signaling pathway to reduce CD14, TLR4, and MMP9 expression during monocyte-to-macrophage differentiation: potential therapeutic implications for atherosclerosis. Antioxidants (Basel). https://doi.org/10.3390/antiox10111798
61. Ren J, Wang Q, Morgan S, Si Y, Ravichander A, Dou C, Kent K, Liu B (2014) Protein kinase C-δ (PKCδ) regulates proinflammatory chemokine expression through cytosolic interaction with the NF-κB subunit p65 in vascular smooth muscle cells. J Biol Chem 289(13):9013–9026. https://doi.org/10.1074/jbc.M113.515957
62. Al Fayi M, Otifi H, Alshyarba M, Dera AA, Rajagopalan P (2020) Thymoquinone and curcumin combination protects cisplatin-induced kidney injury, nephrotoxicity by attenuating NFkappaB, KIM-1 and ameliorating Nrf2/HO-1 signalling. J Drug Target 28(9):913–922. https://doi.org/10.1080/1061186X.2020.1722136
63. Fujikura T, Yasuda H, Iwakura T, Tsuji T, Anders HJ (2019) MDM2 inhibitor ameliorates cisplatin-induced nephropathy via NFkappaBeta signal inhibition. Pharmacol Res Perspect 7(1):e00450. https://doi.org/10.1002/prp2.450
64. Yu C, Dong H, Wang Q, Bai J, Li YN, Zhao JJ, Li JZ (2021) Danshensu attenuates cisplatin-induced nephrotoxicity through activation of Nrf2 pathway and inhibition of NF-kappaB. Biomed Pharmacother 142:111995. https://doi.org/10.1016/j.biopha.2021.111995
65. Yu X, Meng X, Xu M, Zhang X, Zhang Y, Ding G, Huang S, Zhang A, Jia Z (2018) Celastrol ameliorates cisplatin nephrotoxicity by inhibiting NF-kappaB and improving mitochondrial function. EBioMedicine 36:266–280. https://doi.org/10.1016/j.ebiom.2018.09.031

66. Zhang L, Gu Y, Li H, Cao H, Liu B, Zhang H, Shao F (2018) Daphnetin protects against cisplatin-induced nephrotoxicity by inhibiting inflammatory and oxidative response. Int Immunopharmacol 65:402–407. https://doi.org/10.1016/j.intimp.2018.10.018
67. Docherty MH, O'Sullivan ED, Bonventre JV, Ferenbach DA (2019) Cellular senescence in the kidney. J Am Soc Nephrol 30(5):726–736. https://doi.org/10.1681/ASN.2018121251